



Adsorption of lead (Pb²⁺) onto salicylic acid-methanol modified steel slag from aqueous solution: a cost analysis

Ahmad Jonidi Jafari^{a,b}, Mehrdad Moslemzadeh^{b,*}

^aResearch Center for Environmental Health Technology, Iran University of Medical Sciences, Tehran, Iran, Tel. +9886704745/+9886704735; Fax: +982188622707/+982188622712; email: ahmad_jonidi@yahoo.com/jonidi.a@iums.ac.ir (A.J. Jafari)

^bDepartment of Environmental Health Engineering, School of Public Health, Iran University of Medical Sciences, Tehran, Iran, Tel. +9886704745; Fax: +982188622707; email: mehrdad.moslemzadh@gmail.com

Received 5 November 2019; Accepted 10 May 2020

ABSTRACT

Industrial wastewater contaminated with heavy metals is a major environmental and health hazard that can be effectively treated by the absorption process. In this regard, steel slag is a low-cost product used to produce unconventional adsorbents. The present study investigated the applicability of salicylic acid-methanol modified steel slag in the adsorption of lead (Pb²⁺) ion from aqueous solution. Brunauer–Emmett–Teller, scanning electron microscopy, Fourier-transform infrared spectroscopy, and pH_{ZPC} were employed to characterize the synthesized adsorbent. The effects of parameters such as pH, initial concentration, and adsorbent dosage on the adsorption of Pb²⁺ were further examined. With raising the initial concentration of Pb²⁺ to 200.0 mg mL⁻¹, the adsorption capacity increased and then became stable. The increase in adsorbent dosage reduced the adsorption capacity and augmented the removal efficiency. Langmuir isotherm model with $R^2 = 0.9912$ fitted well with the experimental data, and its q_{\max} was 117.6 mg g⁻¹ at pH 7.0. The adsorption process obeyed pseudo-second-order kinetics.

Keywords: Adsorption; Lead (Pb²⁺); Salicylic acid-methanol modified steel slag; Cost analysis

1. Introduction

Many industries, including textile, rubber, paper, leather, plastic, cosmetics, and printing produce large volumes of industrial wastewater that are ultimately discharged into the aquatic environment [1–4]. Discharge of heavy metals in the aquatic environment is hazardous for both toxicological and aesthetic reasons. Heavy metals have long been known to be toxic for human life and the aquatic environment. Widespread in the environment, Pb²⁺ is one of the priority pollutants announced by the US Environmental Protection Agency (USEPA). The occurrence of these pollutants is often associated with human activities such as mining, burning fossil fuels, recycling, and generating lead-acid batteries [5–7]. The increase in the use and production of Pb²⁺ implies

the possibility of its further propagation and distribution in the environment. Pb²⁺ also has a great impact on the human body through oral administration and inhalation among other paths; this pollutant is not easily repelled and accumulates in the body. It can lead to blood disorders, gastrointestinal symptoms such as constipation, nervous system, and kidney problems [8,9]. The USEPA and World Health Organization (WHO) announced that the maximum permitted amount of Pb²⁺ in tap water is 10.0 and 15.0 µg L⁻¹, respectively [10]. Because of the foregoing problems, there has been a growing scientific interest in the development of proper technologies for the removal of Pb²⁺ from different solutions.

Among these technologies, mention can be made of adsorption and ion exchange [11–14], coagulation/flocculation [15–17], precipitation [18–20], and bioaccumulation

* Corresponding author.

[21–23]. However, most of the above methods suffer from one or more limitations. Bioaccumulation is sensitive to the Pb^{2+} concentration [21], and coagulation/flocculation and precipitation generate excessive amounts of sludge [16]. Adsorption is typically employed by wastewater treatment facilities, but it is expensive and hard to regenerate [14,24,25]. Some studies have focused on cost reduction through recovering useful minerals or using industrial byproducts such as steel slag (SS) in water processing. Generated by steel production, steel slag is a high volume solid waste whose annual global production is approximately 170.0–250.0 million metric tonnes/y [26]. SS is mainly composed of CaO , SiO_2 , FeO , Fe_2O_3 , MgO , and MnO . In most cases, the weight of the iron oxides (FeO and Fe_2O_3) is higher than 20.00% in SS [27]. Based on the type of steel and the pretreatment of slag, this byproduct has been categorized as basic oxygen furnace slag, electrical arc furnace slag, blast furnace slag, and casting residue according to the steelmaking process [28]. Many researchers have investigated SS owing to its sufficient ionic contents that can be utilized in the adsorption process [29–31]. SS has been utilized in biological degradation media [32,33], bioremediation [34,35], and adsorption of phosphorus and metals [36–38]. Most of the previous studies focused on the adsorption capacity of SS for the removal of pollutants. There is a large amount of calcium silicate ion in the structure of SS, possibly taking up a high volume of its porosity. Washing SS with chemical removes the calcium silicate ion, thereby increasing its capacity for the adsorption of Pb^{2+} ion. SS also contains certain amounts of iron oxide, hence its magnetic property that can be properly separated by a magnetic field in aqueous solution [27,31]. On the other hand, classical wastewater treatment techniques are costly and require complex installations; therefore, they are not viable in low- and middle-income developing countries. In these cases, the adsorbent process obtained from different industrial by-products can offer technically cost-effective solutions. These substances are chemically active and have a highly porous surface. They also require less processing and have a high adsorption capacity, enabling them to adsorb pollutants from different aqueous solutions in cost-effective ways [39–41].

Therefore, the present study aimed to investigate the adsorption of lead (Pb^{2+}) on salicylic acid-methanol modified steel slag (SAM-modified SS) in aqueous solution and perform a cost analysis to introduce this adsorbent as economic. The effects of pH, adsorbent dosage, and Pb^{2+} concentration were further examined regarding the removal of Pb^{2+} from aqueous solution. Moreover, adsorption isotherm, kinetic processes, and reusability of SAM-modified SS were studied, and a cost analysis was finally conducted.

2. Materials and methods

2.1. Chemicals

Tap water was used to prepare the test solution characterized in Table S1. Pb^{2+} (lead nitrate at 99.999% purity) was purchased from Aldrich, USA. The test solution containing Pb^{2+} for the experiments was prepared by suitable dilution of the standard lead nitrate solution (concentration 1,000 mg L^{-1}) with distilled water. The SS was obtained from a steel production facility in Yazd Province, Iran, and

its composition was determined using an X-ray fluorescent quantometer type “ARL-72000 S” (Table 1). Other chemicals used in the experiments were of analytical grade methanol (chromatographic grade), salicylic acid (Sigma-Aldrich, USA > 90.00%) NaCl (Merck, Suprapur, 99.60%), HCl (Merck, Germany, Germany, Suprapur), NaOH pellets (Merck, Germany, Suprapur > 99.00%), and HNO_3 (VWR Prolabo, 69.40% for cleaning, and Merck (Germany), Suprapur for AAS measurements). Milli-Q 18 M Ω water was used in all solution preparations.

2.2. Salicylic acid-methanol modified SS preparation

The salicylic acid-methanol solution was prepared by dissolving 10.0 g salicylic acid in 100.0 mL methanol solvent. Afterward, the SS was washed with distilled water to remove surface impurities and dried at 100.0°C for 24 h. ultimately, it was crushed and ground with a planetary ball mill (YXQMO-4L, MITR, China) and sieved for a 200 mesh size. Using ultrapure water, the obtained SS powder was washed again for many times and then dried. 200.0 g of the dried SS powder was added into 100.0 mL SAM solution (100.0 g L^{-1}) and shaken on a shaking bed with a constant shaking rate of 200 rpm min^{-1} at 25.0°C for 6 h. Next, the powder was separated from the suspension by a magnet (1.5 Tesla). The residues were washed repeatedly by ultrapure water. After the drying step (at 90.0°C in the oven for 12 h), the SAM-modified SS adsorbent (SAM-modified SS) was obtained [31].

2.3. Experimental

The adsorption of Pb^{2+} by SAM-modified SS was investigated in the batch experiments using 250 conical flasks containing 100 mL of Pb^{2+} ion solution under atmospheric conditions. This was done to measure the adsorption efficiency of the produced adsorbent for Pb^{2+} as a function of pH (3.0, 4.0, 5.0, 6.0, 7.0, and 8.0), Pb^{2+} concentration (50.0, 100.0, 150.0, 200.0, and 300.0 mg L^{-1}), adsorbent dosage (0.1, 0.4, 0.8, 1.2, and 1.6 g), agitation time (90 min), and 25.0°C.

Pb^{2+} concentrations were measured by furnace atomic absorption spectroscopy (AAS 220 Z, Spectra AA). The samples were treated with acid (2.00% HNO_3) prior to the final analysis. The amount of Pb^{2+} adsorbed per unit mass of SAM-modified SS (adsorbent) and the removal rate was calculated as follows:

Table 1
Steel slag characterization

Ingredient	Content %
MnO	3.52
Fe_2O_3	39.52
Al_2O_3	0.21
SiO_2	12.32
CaO	32.65
MgO	9.53
Cr_2O_7	0.20
Others	2.05

$$\text{Removal efficiency (\%)} = \frac{C_i - C_e}{C_i} \times 100 \quad (1)$$

While the adsorption capacity of adsorbent was calculated using the following equation:

$$q_t (\text{mg L}^{-1}) = \frac{(C_i - C_e)V}{M} \quad (2)$$

where C_i and C_e are the initial and equilibrium concentrations of Pb^{2+} ion (mg L^{-1}), q_e is the capacity of adsorption (mg g^{-1}), V represents the volume of Pb^{2+} ion solution (L), and M is the mass of adsorbent (g).

2.4. Adsorbent characteristics

The SS and SAM-modified SS were characterized through the use of Fourier-transform infrared spectroscopy (FTIR), scanning electron microscopy (SEM), and zeta potential analyses. Furthermore, the specific surface area, pore size and pore volume of SS, and SAM-modified SS were obtained by the Brunauer–Emmett–Teller (BET) adsorption method (Micromeritics Instrument Corporation, TRI-STAR3020, USA) [42,43].

2.5. pH at the point of zero charge

The following steps were performed to determine the pH at the point of zero charge (pH_{PZC}) for SAM-modified SS powder: primarily, a sufficient amount of 0.1 M NaCl solution was poured into 250 mL flasks, and the pH was adjusted to 2.0–11.0 by either 1 M HCl or NaOH. After that, the total volume of the solution in each flask was adjusted to 100.0 mL via adding NaCl solution of the same known

concentration; simultaneously, the initial pH values of the solutions were accurately noted. In the next step, 0.4 g of SAM-modified SS powder was added to the flasks, and the suspensions were then shaken and allowed to equilibrate for 24 h by a shaker. Lastly, the final pH values of the supernatant suspension were noted. The analyzed results are shown in Fig. 4b, where the pH_{PZC} of the AB SAM-modified SS was found to be 4.0 [25].

2.6. Desorption experiments

0.5 g of the Pb^{2+} -loaded (SAM-modified SS) adsorbent was shaken with 50.0 mL of 1.0 M HCl as a desorbing agent in a 250 mL conical flask on a reciprocating shaker with a rotation speed of 220 rpm at 25°C for 24 h. The suspension was centrifuged and the supernatant solution was filtered prior to Pb^{2+} analysis using an AAS [43].

3. Results and discussion

3.1. Adsorbent characteristics

As presented in Table S2, BET analysis showed that the average specific surface areas of SS and SAM-modified SS were 6.33 and 62.82 $\text{m}^2 \text{g}^{-1}$, respectively. However, modification with SAM significantly increased the average specific surface area of the SS. As it is shown in Table 1, a major amount of SS belonged to the CaO and MgO. After washing the SS with chemicals, the mentioned salt was dissolved so that the occupied pores reappeared [44]. Additionally, the pore size and the total pore volume of SAM-modified SS were determined to be 50.0 nm and $3.6 \times 10^{-3} \text{ cm}^3 \text{ g}^{-1}$, respectively. The BET analysis showed that the modified SS had a high adsorption capacity. SEM analysis was further performed to study the morphological changes in the SS

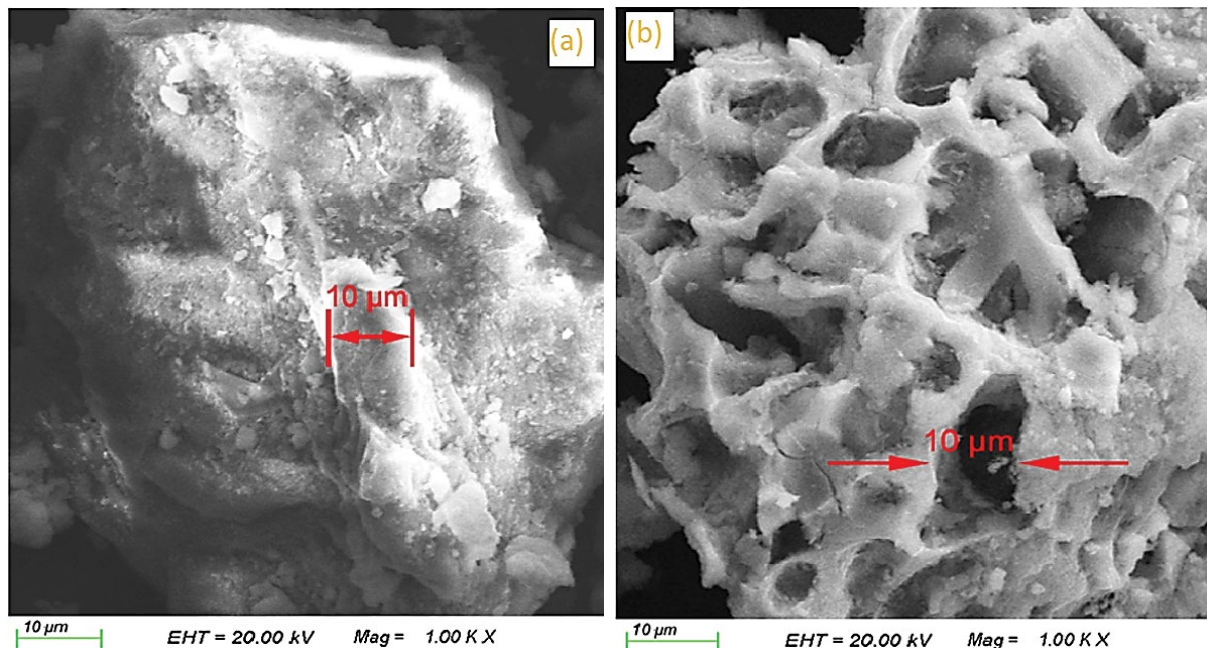


Fig. 1. SEM studies of the samples.

(Figs. 1a and b). The surface of the untreated SS was relatively flat, smooth, and uniform. As can be seen, the surface morphology of the SS was significantly changed after chemical modification with SAM. The external surface area was noticeably increased by the formation of more pores (Fig. 1). The significant increase in pores was probably due to the dissolution of the calcium silicate minerals in the SS by SAM treatment. FTIR spectra of the samples were utilized to further study the adsorption of Pb^{2+} by the SAM-modified SS. The FTIR spectra of the SS and the SAM-modified SS were prepared as shown in Fig. 2. The broad bands in the range $1,400\text{--}1,500\text{ cm}^{-1}$ (Ca–O) and $800\text{--}1,000\text{ cm}^{-1}$ (Si–O) were related to the typical stretching vibrations of Ca–O and Si–O, respectively [45,46].

3.2. Effect of agitation time and equilibrium

The effect of agitation time on adsorption efficiency was investigated under both tap water and deionized water conditions: $\text{pH} = 7.0$, $\text{Pb}^{2+} = 500.0\text{ mg L}^{-1}$, adsorbent dosage = 0.1 g , room temperature, and 200 min time. The results are illustrated in Fig. 3. Concerning tap water, the adsorption of Pb^{2+} increased rapidly in the first 40 min and then increased slowly between 30 and 70 min . After 70 min , the adsorption capacity reached a maximum and then remained steady, at which point, the adsorption capacity at equilibrium was 112.0 mg g^{-1} . Regarding deionized water, the adsorption system reached an equilibrium in the first 50 min , where the maximum adsorption capacity was 121.0 mg g^{-1} . The increased adsorption capacity and the reduced equilibrium time can be the result of the interfering ions existing in the tap water [25]. However, we used tap water for further experiments.

3.3. Effect of pH

To investigate the effect of pH on the adsorption of Pb^{2+} on the SAM-modified SS, Pb^{2+} adsorption experiments

were performed under the following conditions: the initial pH of the Pb^{2+} solution was $3.0\text{--}8.0$, the Pb^{2+} concentration was 150.0 mg L^{-1} , the adsorbent dosage was 0.1 g , and the temperature and time were 25.0°C and 70 min . The results of pH evolution and pH_{ZPC} are shown in Figs. 4a and b. As observed in Fig. 4b, the surface charge of the SAM-modified SS powder became zero at $\text{pH} = 4.0$. Similarly, Zhang reported that it was only at acidic pH that the surface of the SAM-modified SS powder was protonated with H^+ . Above the pH_{ZPC} (4.0), the surface charge of SAM-modified SS powder was negative, adsorbing Pb^{2+} with a positive charge. Based on the results of Fig. 4a, the amount of the adsorbed Pb^{2+} tended to increase with raising the pH from 3.0 to 7.0 , after which the adsorption amount was reduced. The maximum adsorption capacity (49.87 mg g^{-1}) was observed at $\text{pH} 7.0$, which is in line with many studies where the adsorption equilibrium and maximum adsorption capacity occurred at $\text{pH} 7.0$ [47–49]. When the pH value was higher

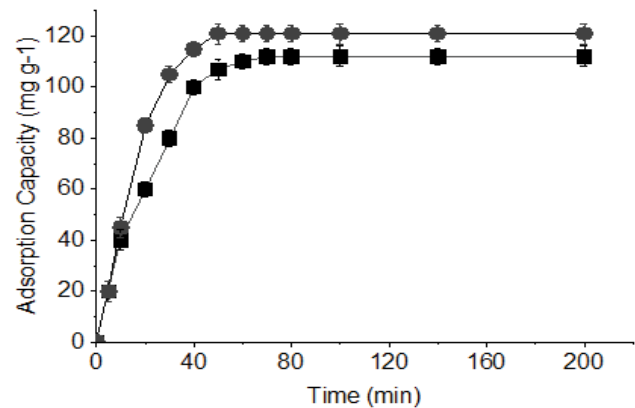


Fig. 3. Effect of agitation time on the adsorption process ($[\text{Pb}^{2+}]$ concentration of 500.0 mg L^{-1} ; 0.4 g adsorbent dosage; 25.0°C ; 200 min).

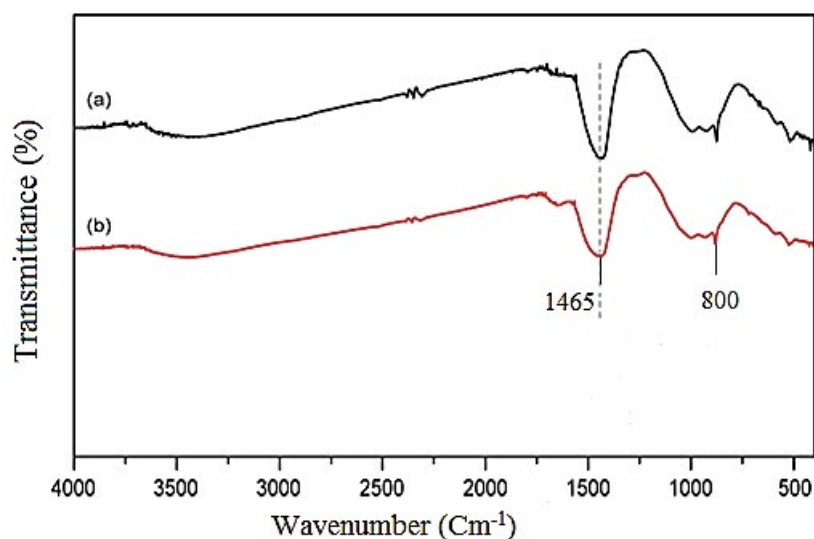


Fig. 2. FTIR spectra of the samples.

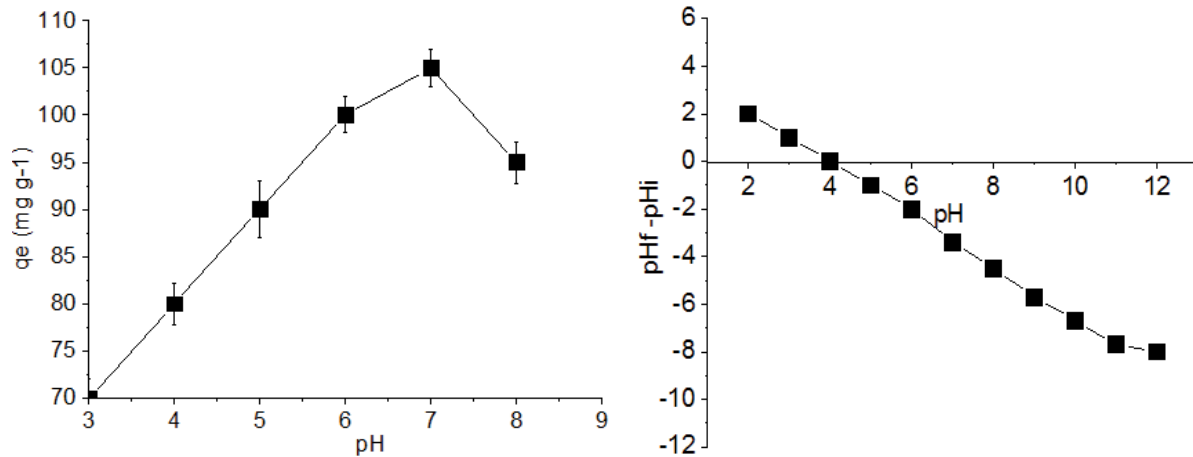


Fig. 4. Effect of the pH values of the Pb^{2+} solution on the adsorption process ($[\text{Pb}^{2+}]$ concentration of 150.0 mg L^{-1} ; 0.1 g adsorbent dosage; 25.0°C ; 120 min).

than 7.0, the Pb^{2+} ion formed a complex with the hydroxide ion to form precipitation, making it difficult to accurately measure the adsorbed amount [49]. At low pH, the amount of adsorption (37.50 mg g^{-1}) was thought to be lower because of competitive adsorption between Pb^{2+} and H^+ ions [36,50].

3.4. Effect of dosage

A SAM-modified SS dosage range of $0.1\text{--}1.6 \text{ g}$ was used to specify the optimum metal adsorption mass of the adsorbent. For this purpose, $0.1, 0.4, 0.8, 1.2,$ or 1.6 g of the SAM-modified SS were prepared for each adsorption experiment. The experiments examined the solutions containing 150.0 mg L^{-1} Pb^{2+} with different masses of SAM-modified SS ($0.1\text{--}1.6 \text{ g}$) at a pH of 7.0 (Fig. 5). As seen, the adsorption capacity and the removal efficiency of the adsorbent showed a reverse tendency with the increase in adsorbent mass. Adsorbed Pb^{2+} per mass of the adsorbent decreased from 105.0 to 9.3 mg g^{-1} with increasing the dose from 0.1 g to 1.6 g ; the removal efficiency increased from 70.00% to 99.96% owing to the presence of highly unoccupied sorption sites at a higher adsorbent mass, where the concentration of Pb^{2+} is constant. An increase in the adsorbent mass could augment the removal efficiency in the process because of the increase in the adsorbent surface and the concentration constant of Pb^{2+} in solution. Similar behavior was reported for Pb^{2+} ion by Liu et al. [36] and Mercado-Borraro et al. [51].

3.5. Effect of Pb^{2+} concentration

Samples were prepared to specify the adsorption efficiency of the SAM-modified SS with different concentrations of Pb^{2+} ion. A certain amount of the SAM-modified SS (0.1 g) was mixed with 100.0 ml of the Pb^{2+} solution ($50.0\text{--}300.0 \text{ mg L}^{-1}$) at pH 7.0. The samples were shaken for 70 min , and the obtained results are shown in Fig. 6. The amount of the adsorbed Pb^{2+} tended to increase with the rise in the initial concentration, and the maximum adsorption 112.0 mg g^{-1} occurred at an initial concentration of 200.0 mg L^{-1} . At initial Pb^{2+} concentrations higher

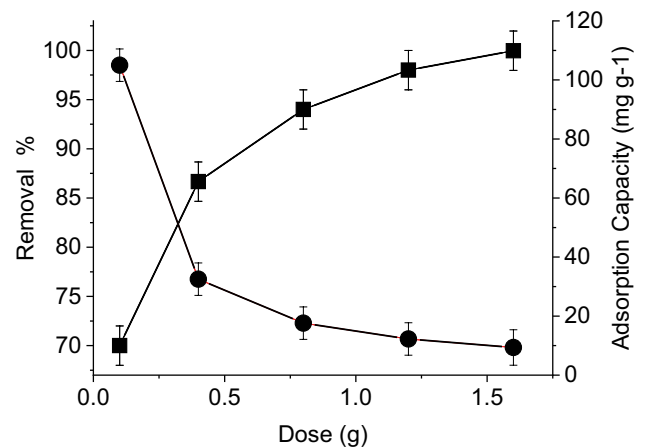


Fig. 5. Effect of the dosage of adsorbent on the adsorption process (pH = 7.0; $[\text{Pb}^{2+}]$ concentration of 150.0 mg L^{-1} ; 25.0°C ; 70 min).

than 200.0 mg L^{-1} , an increase was observed in the adsorption amount (Fig. 6). At a defined adsorbent dosage, the removal of Pb^{2+} depends on the initial concentration of Pb^{2+} because the increase in Pb^{2+} concentration reduces the available adsorption sites. The electrostatic repulsion forces between the adsorbed negatively-charged Pb^{2+} ions further reduced the adsorption [4].

3.6. Isotherm studies

Adsorption isotherm was used to investigate the distribution of Pb^{2+} ion on the SAM-modified SS at equilibrium. The relationship between Pb^{2+} concentration in the solution and the adsorbed Pb^{2+} ion was determined by the use of the Langmuir and Freundlich isotherms [4,25].

The Langmuir isotherm assumes that the active site on the SAM-modified SS surface has the same energy, and the adsorption occurs through the formation of a monolayer on the SAM-modified SS surface. The Langmuir model equation is as follows:

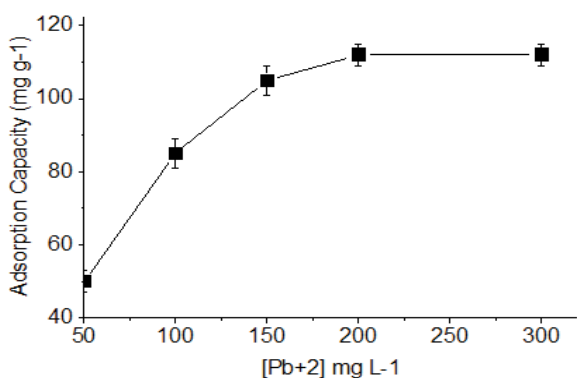


Fig. 6. Effect of Pb²⁺ concentration on the adsorption process (pH = 7.0; 0.1 g dosage; 25.0°C; 70 min).

$$\frac{1}{q_e} = \frac{1}{k_L q_m C_e} + \frac{1}{q_m} \quad (3)$$

The Langmuir constants (q_m , k_L and C_e) are related to maximum adsorption capacity (mg g^{-1}), and the energy of adsorption (L mg^{-1}) and the equilibrium concentration of Pb^{2+} ion in solution (L mg^{-1}) are calculated from the plot $1/q_e$ vs. $1/C_e$ respectively.

R_L , the separation factor, is defined by Eq. (4).

$$R_L = \frac{1}{1 + k_L C_0} \quad (4)$$

where R_L is a dimensionless constant and C_0 is the initial Pb^{2+} ion concentration (mg L^{-1}).

The Freundlich isotherm takes into account the heterogeneity of the SAM-modified SS surface and the existing interactions between the adsorbed Pb^{2+} ions. The Freundlich model equation as follows

$$\ln q_e = \ln k_f + \frac{1}{n} (\ln C_e) \quad (5)$$

Table 2
Results of adsorption isotherm

Langmuir isotherm	Parameters	Freundlich isotherm	Parameters
0.17	k_L (L mg^{-1})	6.0	k_f (mg g^{-1})
117.6	q_m (mg g^{-1})	2.1	n
0.03	R_L	0.9127	R^2
0.9912	R^2		

where k_f and n , Freundlich constants, represent adsorption capacity (mg g^{-1}) and the adsorption intensity of system determined from the plot of $\ln q_e$ vs. $\ln C_e$.

In this case, the coefficient of determination (R^2) of the Langmuir isotherm model (0.9912) was higher than the Freundlich isotherm model (0.9127) (Fig. 7a). This result indicates that the surface of the SAM-modified SS was uniform, and a monolayer of the adsorbate was formed when adsorption reached equilibrium. Other parameters of the models are shown in Table 2. As seen, Langmuir constants q_{max} , k_L , and R_L were 117.6 mg g^{-1} , 0.17 L mg^{-1} , and 0.03 , respectively. R_L , the relative volatility in the vapor-liquid equilibrium, is easy to verify because it ranges from 1 to 0 for a favorable equilibrium, and it is larger than 1 for an unfavorable equilibrium [4]. In our study, R_L varied between 0 and 1, implying a favorable adsorption process. Furthermore, the Freundlich constants (k_f and n) calculated from the plot of $\ln q_e$ vs. $\ln C_e$ (not provided here) were 6.0 mg g^{-1} and 2.1 , respectively (Table 2). The value of n was larger than 1, indicating a favorable adsorption system and a physical process [4]. In some studies, the researchers observed that the model properly described the adsorption isotherm of Pb^{2+} ion on the adsorbents [46,52]. Table 3 compares the present study with others regarding the maximum adsorption capacity of Pb^{2+} ion with various adsorbents. Liu et al. [37] reported 13.2 mg g^{-1} as q_{max} for adsorption of Pb^{2+} on the untreated SS (Table 3). The comparison showed that the SAM-modified SS had a higher adsorption capacity, hence considered as a promising adsorbent for the removal of Pb^{2+} ion from aqueous solution.

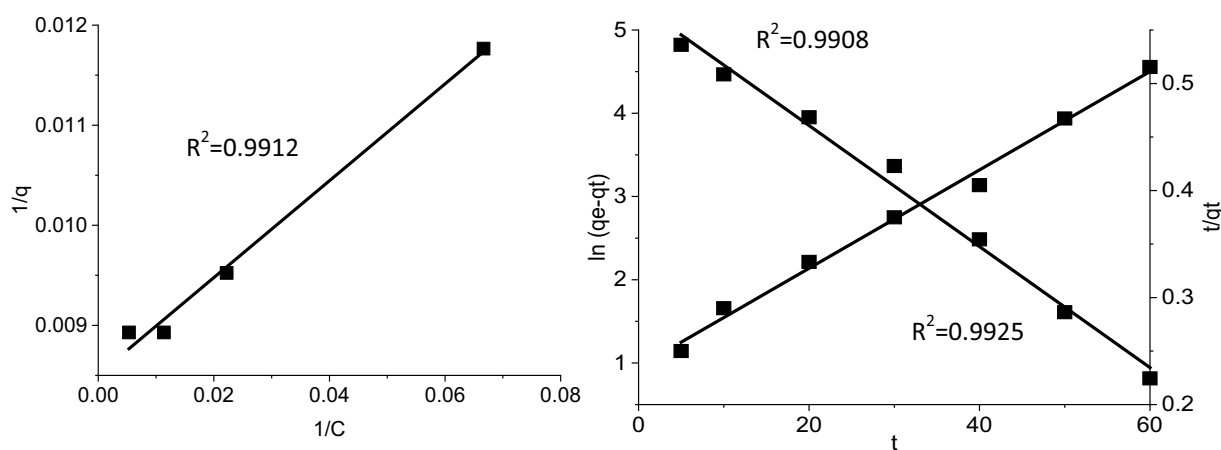


Fig. 7. Plots of isotherm (a) and kinetics (b) studies.

Table 3
Comparison of the maximum adsorption capacity of Pb²⁺

Studies	q_{\max} (mg g ⁻¹)
This study	117.6
Untreated SS [37]	13.2
Reduced graphene oxides (rGO) [42]	95.0
Pristine rice husks [53]	1.9
Functionalized cryogels [54]	172.4
Modified biochar (rape straw and orthophosphate) [46]	38.1
Modified biochar (coconut fibre) [43]	85.2

3.7. Kinetic studies

To study the mechanisms of adsorption which control the adsorption behavior, two well-known kinetic models, pseudo-first-order and pseudo-second-order [34,55] rate equations, were applied to fit the data. Their linear forms are presented in Eqs. (6) and (7):

$$\ln(q_e - q_t) = \ln q_e - k_1 t \quad (6)$$

$$\frac{t}{q_t} = \frac{1}{k_2 q_e^2} + \frac{1}{q_e} t \quad (7)$$

where q_e (mg g⁻¹) and q_t (mg g⁻¹) are the amounts of Pb²⁺ ion adsorbed at equilibrium, and t is the contact time (min). k_1 (min⁻¹) and k_2 (g mg⁻¹ min⁻¹) are the rate constants of the pseudo-first and second-order kinetics, respectively.

Fig. 7b shows the plot of t/q_t vs. t from the pseudo-second-order kinetic. Other parameters of both kinetic models are presented in Table 4. According to the results, pseudo-second-order kinetic with a good coefficient of determination ($R^2 = 0.9925$) was a better fit compared with pseudo-first-order kinetic ($R^2 = 0.9508$). Several studies have reported this behavior for Pb²⁺ ion adsorbed on other adsorbents [36,56]. In addition, the pseudo-second-order kinetic

model predicted a significantly high value of equilibrium adsorption capacity (q_{ecal}) closer to the experimental (q_e) value, indicating the applicability of this model (Table 4); the theoretical q_e (q_{ecal}) values in pseudo-first-order kinetic were much lower than the experimental q_e values (Table 4). Also, pseudo-second-order kinetic had a high adsorption rate constant (k_2). Based on this model, two reactions occur either in series or in parallel. The first reaction quickly reaches equilibrium while the second one is slower and can last for a long period of time [57]. Therefore, it can be concluded that the pseudo-second-order kinetic model better described the mechanism and behavior associated with the adsorption of Pb²⁺ ion onto the SAM-modified SS adsorbent.

3.8. Reusability study

Desorption is an important factor that enables the recycling of metal ions and adsorbents. In this way, adsorbent recycling contributes to the economic sustainability of adsorption-based treatment systems. In recent studies, numerous chemicals have been applied as desorption process agents. These agents are to be selected carefully due to the permanent structural changes and adsorption capacity reductions that different chemicals can induce in adsorbent materials [31]. In the present study, desorption of Pb²⁺ from SAM-modified SS was carried out by 1 M HCl solution, summarized in Fig. 8a. As observed, the performance of the SAM-modified SS had a constant value of 86.00 % even after five cycles of use. The specific surface area of the SAM-modified SS was also specified following five cycles of use. Table S2 shows that the specific surface area decreased after regeneration, explaining the reduced performance of the adsorbent. Given the acceptable performance after four cycles of use, it is safe to say that the commercial use of SAM-modified SS might be economical as far as reusability is concerned.

3.9. Application in industrial wastewater

To study the removal efficiency in practice, real wastewater containing chromium provided by a local industrial

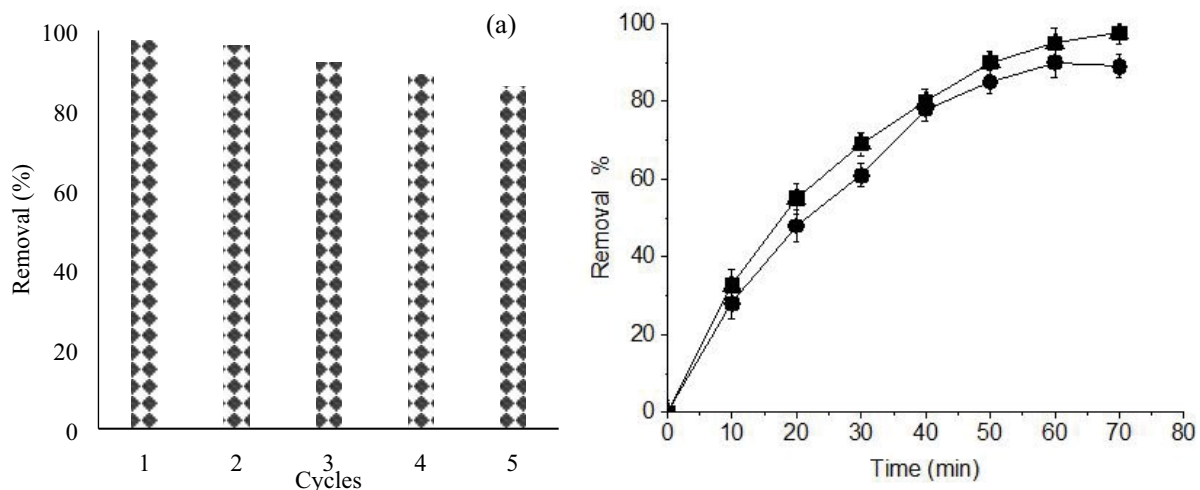


Fig. 8. Regeneration experiment of SAM-modified SS (a) and application in real wastewater (b).

Table 4
Results of adsorption kinetics

Kinetic parameters	q_e (mg g ⁻¹) exp.	q_e (mg g ⁻¹) cal.	k_1 (min ⁻¹)	k_2 (g mg ⁻¹ min ⁻¹)	R^2
Pseudo-first-order	112.0	77.2	1.6		0.9508
pseudo-second-order	112.0	108.3		8.01	0.9925

Table 5
Cost of preparing 1 kg of adsorbents

Materials	Unit cost (US\$ kg ⁻¹)	Adsorbent	
		Amount used (kg)	Cost (US\$ kg ⁻¹)
Steel slag	6 (1,000 kg)	1	0.006
Methanol	36	0.500	17.5
Salicylic acid	47	0.150	7
Cost of grinding	24	1	24
Cost of drying	2	1	2
Total cost (IRR)			50.506

park in Yazd providence was used in this study. The wastewater was naturally acidic and comprised of various toxic substances, including heavy metals such as chromium and nickel, organic compounds, and inorganic phosphorus compounds (Table S3). The adsorption process was done for both the synthetic wastewater and the real wastewater under the following conditions; pH = 7.0, 1.0 g adsorbent dosage, and Pb²⁺ concentration of 208.0 mg L⁻¹ in 1.0 L sample. Fig. 8b shows no significant decrease in the removal efficiency in the tap water experiment compared to the industrial wastewater experiment. The removal efficiency in the tap water and industrial wastewater experiments was 97.59% with an adsorption capacity of 112.0 mg L⁻¹, and 89.00% with an adsorption capacity of 104.0 mg L⁻¹, respectively. Previous studies examined the removal of organics and inorganics by the use of steel slag which was shown to have a lower tendency to adsorb organic compounds compared with metals [58,59]. In the current study, organics probably could not occupy SAM-modified SS, hence the adsorption of metals on SAM-modified SS. On the other hand, the maximum adsorption capacity obtained in this study belonged to the tap water which was similar to the industrial wastewater regarding interfering ions. In this view, SAM-modified SS might have sufficiently adsorbed Pb²⁺ in the industrial wastewater. However, SAM-modified SS was proven an efficient adsorbent for Pb²⁺ in synthetic wastewater as well as real wastewater.

3.10. Cost analysis in industrial wastewater

The present study focused on the preparation of SAM-modified SS and its use for the removal of Pb²⁺ ions from aqueous solution. The overall cost comprises various parameters such as the collection source, preparation methodology, and subsequent treatment [60]. Hence, an attempt was made to analyze the cost of modified SS adsorbent and the utilized chemicals. Table 5 shows the

cost of all activities including physical and chemical activation processes and the overall preparation cost of SAM-modified SS. The total cost for the preparation of 1 kg of adsorbent was estimated at 50.506 USD. As seen in Table 5, raw SS had a low price in Iran, but it was annually produced in high amounts; therefore, it can be economical and cost-effective to use SS as Pb²⁺ adsorbent. Based on the adsorption capacity obtained from the batch studies for the SAM-modified SS (104.0 mg g⁻¹), the adsorbent cost 1 USD to remove 1 g of Pb²⁺ from the industrial wastewater stream.

4. Conclusion

The present work reported the preparation of SAM-modified SS for the removal of Pb²⁺ ions from aqueous solution. The prepared SAM-modified SS exhibited a high surface area and a good adsorption ability to remove Pb²⁺ at natural pH values. Hence, SAM-modified SS can be considered as a low-cost and applicable adsorbent for the removal of Pb²⁺ ions. Moreover, the fabricated SAM-modified SS could be an economical alternative for the removal of Pb²⁺ ions from aqueous solution and real wastewater. The maximum adsorption capacity was 117.6 mg g⁻¹. The adsorption kinetics and isotherm studies revealed that the adsorption of the SAM-modified SS followed the pseudo-second-order model and the Langmuir isotherm model. It seems the adsorption process fitted the mono-layer adsorption model and followed the mechanism of chemisorption in nature through exchanging electrons or sharing valence forces between the SAM-modified SS and Pb²⁺ ions. The industrial wastewater experiment implied that the SAM-modified SS is an effective adsorbent for the treatment of industrial wastewater and removal of Pb²⁺ ions. As a renewable, low-cost, and environment-friendly material, the SAM-modified SS could be easily chemically modified. It also exhibited excellent adsorption ability towards Pb²⁺ ions in aqueous solutions, showing a

promising economical and practical application in wastewater purification.

Acknowledgment

The authors acknowledge Iran University of Medical Sciences for financial support. We also acknowledge the School of Health for providing research facilities.

References

- [1] A.J. Jafari, M. Mahrooghi, M. Moslemzadeh, Removal of *Escherichia coli* from synthetic turbid water using titanium tetrachloride and zirconium tetrachloride as coagulants, *Desal. Water Treat.*, 163 (2019) 358–365.
- [2] H. Pasalari, H.R. Ghaffari, A.H. Mahvi, M. Pourshabani, A. Azari, Activated carbon derived from date stone as natural adsorbent for phenol removal from aqueous solution, *Desal. Water Treat.*, 72 (2017) 406–417.
- [3] K. Taghavi, D. Naghipour, A. Mohagheghian, M. Moslemzadeh, Photochemical degradation of 2,4-dichlorophenol in aqueous solutions by Fe²⁺/peroxydisulfate/UV process, *Int. J. Eng.*, 30 (2017) 15–22.
- [4] D. Naghipour, K. Taghavi, M. Moslemzadeh, Removal of methylene blue from aqueous solution by artist's bracket fungi: kinetic and equilibrium studies, *Water Sci. Technol.*, 73 (2016) 2832–2840.
- [5] N.J. Li, G.M. Zeng, D.L. Huang, C. Huang, C. Lai, Z. Wei, P. Xu, C. Zhang, M. Cheng, M. Yan, Response of extracellular carboxylic and thiol ligands (oxalate, thiol compounds) to Pb²⁺ stress in *Phanerochaete chrysosporium*, *Environ. Sci. Pollut. Res.*, 22 (2015) 12655–12663.
- [6] X.K. Kong, G.X. Huang, Z.T. Han, Y.M. Xu, M. Zhu, Z.J. Zhang, Evaluation of zeolite-supported microscale zero-valent iron as a potential adsorbent for Cd²⁺ and Pb²⁺ removal in permeable reactive barriers, *Environ. Sci. Pollut. Res.*, 24 (2017) 13837–13844.
- [7] K. Huang, H.M. Zhu, Removal of Pb²⁺ from aqueous solution by adsorption on chemically modified muskmelon peel, *Environ. Sci. Pollut. Res.*, 20 (2013) 4424–4434.
- [8] R. Ahmad, R. Kumar, M.A. Laskar, Adsorptive removal of Pb²⁺ from aqueous solution by macrocyclic calix[4]naphthalene: kinetic, thermodynamic, and isotherm analysis, *Environ. Sci. Pollut. Res.*, 20 (2013) 219–226.
- [9] J. Tang, C.X. Chen, L. Chen, M. Daroch, Y. Cui, Effects of pH, initial Pb²⁺ concentration, and polyculture on lead remediation by three duckweed species, *Environ. Sci. Pollut. Res.*, 24 (2017) 23864–23871.
- [10] Y.-J. Tu, C.-F. You, M.-H. Chen, Y.-P. Duan, Efficient removal/recovery of Pb onto environmentally friendly fabricated copper ferrite nanoparticles, *J. Taiwan Inst. Chem. Eng.*, 71 (2017) 197–205.
- [11] Q.M. Wang, L. Peng, Y.Y. Gong, F.F. Jia, S.X. Song, Y.M. Li, Mussel-inspired Fe₃O₄/polydopamine(PDA)-MoS₂ core-shell nanosphere as a promising adsorbent for removal of Pb²⁺ from water, *J. Mol. Liq.*, 282 (2019) 598–605.
- [12] M. Izanloo, A. Esrafil, A.J. Jafari, M. Farzadkia, M. Behbahani, H.R. Sobhi, Application of a novel bi-functional nanoadsorbent for the simultaneous removal of inorganic and organic compounds: equilibrium, kinetic and thermodynamic studies, *J. Mol. Liq.*, 273 (2019) 543–550.
- [13] D. Wu, Y.G. Wang, Y. Li, Q. Wei, L.H. Hu, T. Yan, R. Feng, L.G. Yan, B. Du, Phosphorylated chitosan/CoFe₂O₄ composite for the efficient removal of Pb(II) and Cd(II) from aqueous solution: adsorption performance and mechanism studies, *J. Mol. Liq.*, 277 (2019) 181–188.
- [14] K. Naseem, R. Begum, W.T. Wu, M. Usman, A. Irfan, A.G. Al-Sehemi, Z.H. Farooqi, Adsorptive removal of heavy metal ions using polystyrene-poly(*N*-isopropylmethacrylamide-acrylic acid) core/shell gel particles: adsorption isotherms and kinetic study, *J. Mol. Liq.*, 277 (2019) 522–531.
- [15] A.J. Hargreaves, P. Vale, J. Whelan, L. Alibardi, C. Constantino, G. Dotro, E. Cartmell, P. Campo, Impacts of coagulation-flocculation treatment on the size distribution and bioavailability of trace metals (Cu, Pb, Ni, Zn) in municipal wastewater, *Water Res.*, 128 (2018) 120–128.
- [16] A.J. Bora, R.K. Dutta, Removal of metals (Pb, Cd, Cu, Cr, Ni, and Co) from drinking water by oxidation-coagulation-adsorption at optimized pH, *J. Water Process Eng.*, 31 (2019) 100839.
- [17] H.S. Kim, B.-H. Seo, S. Kuppusamy, Y.B. Lee, J.-H. Lee, J.-E. Yang, G. Owens, K.-R. Kim, A DOC coagulant, gypsum treatment can simultaneously reduce As, Cd and Pb uptake by medicinal plants grown in contaminated soil, *Ecotoxicol. Environ. Saf.*, 148 (2018) 615–619.
- [18] M.Y. Ye, G.J. Li, P.F. Yan, L. Zheng, S. Sun, S.S. Huang, H.F. Li, Y. Chen, L.K. Yang, J.L. Huang, Production of lead concentrate from bioleached residue tailings by brine leaching followed by sulfide precipitation, *Sep. Purif. Technol.*, 183 (2017) 366–372.
- [19] L. Di Palma, P. Ferrantelli, C. Merli, F. Biancifiore, Recovery of EDTA and metal precipitation from soil flushing solutions, *J. Hazard. Mater.*, 103 (2003) 153–168.
- [20] J.L. Conca, J. Wright, An Apatite II permeable reactive barrier to remediate groundwater containing Zn, Pb and Cd, *Appl. Geochem.*, 21 (2006) 1288–1300.
- [21] I.C. Bordon, A.K. Emerenciano, J.R.C. Melo, J.R.M.C. da Silva, D.I.T. Favaro, P.K. Gusso-Choueri, B.G. de Campos, D.M. de Souza Abessa, Implications on the Pb bioaccumulation and metallothionein levels due to dietary and waterborne exposures: the *Callinectes danae* case, *Ecotoxicol. Environ. Saf.*, 162 (2018) 415–422.
- [22] N. Urien, A. Farfarana, E. Uher, L.C. Fechner, A. Chaumot, O. Geffard, J.D. Lebrun, Comparison in waterborne Cu, Ni and Pb bioaccumulation kinetics between different gammarid species and populations: natural variability and influence of metal exposure history, *Aquat. Toxicol.*, 193 (2017) 245–255.
- [23] R. Hadji, N. Urien, E. Uher, L.C. Fechner, J.D. Lebrun, Contribution of aqueous and dietary uptakes to lead (Pb) bioaccumulation in *Gammarus pulex*: from multipathway modeling to in situ validation, *Ecotoxicol. Environ. Saf.*, 129 (2016) 257–263.
- [24] G. Durán-Jiménez, V. Hernández-Montoya, J. Rodríguez Oyarzun, M.A. Montes-Morán, E. Binner, Pb(II) removal using carbon adsorbents prepared by hybrid heating system: Understanding the microwave heating by dielectric characterization and numerical simulation, *J. Mol. Liq.*, 277 (2019) 663–671.
- [25] S. Pourkarim, F. Ostovar, M. Mahdavianpour, M. Moslemzadeh, Adsorption of chromium(VI) from aqueous solution by artist's bracket fungi, *Sep. Sci. Technol.*, 52 (2017) 1733–1741.
- [26] H.I. Gomes, W.M. Mayes, H.A. Baxter, A.P. Jarvis, I.T. Burke, D.I. Stewart, M. Rogerson, Options for managing alkaline steel slag leachate: a life cycle assessment, *J. Cleaner Prod.*, 202 (2018) 401–412.
- [27] M. Cheng, G.M. Zeng, D.L. Huang, C. Lai, Y. Liu, P. Xu, C. Zhang, J. Wan, L. Hu, W.P. Xiong, C.Y. Zhou, Salicylic acid-methanol modified steel converter slag as heterogeneous Fenton-like catalyst for enhanced degradation of alachlor, *Chem. Eng. J.*, 327 (2017) 686–693.
- [28] H. Yi, G.P. Xu, H.G. Cheng, J.S. Wang, Y.F. Wan, H. Chen, An overview of utilization of steel slag, *Procedia Environ. Sci.*, 16 (2012) 791–801.
- [29] B.M. Sellner, G.H. Hua, L.M. Ahiablame, T.P. Trooien, C.H. Hay, J. Kjaersgaard, Evaluation of industrial by-products and natural minerals for phosphate adsorption from subsurface drainage, *Environ. Technol.*, 40 (2019) 756–767.
- [30] V.T. Le, V.D. Doan, D.D. Nguyen, H.T. Nguyen, Q.P. Ngo, T.K.N. Tran, H.S. Le, A novel cross-linked magnetic hydroxyapatite/chitosan composite: preparation, characterization, and application for Ni(II) Ion removal from aqueous solution, *Water Air Soil Pollut.*, 229 (2018), doi: 10.1007/s11270-018-3762-9.
- [31] M. Cheng, G.M. Zeng, D.L. Huang, C. Lai, Y. Liu, C. Zhang, R.Z. Wang, L. Qin, W.J. Xue, B. Song, S.J. Ye, H. Yi, High adsorption of methylene blue by salicylic acid-methanol modified steel converter slag and evaluation of its mechanism, *J. Colloid Interface Sci.*, 515 (2018) 232–239.

- [32] Z.P. Wang, Y.Z. Guo, Y.Q. Chen, S.W. Liang, J.L. Zuo, X.W. Yu, Simulated sunlight enhanced X3B degradation by persulfate activated with steel slag, 142 (2016) 1–7, doi: 10.1061/(ASCE)EE.1943-7870.0001002.
- [33] Y.J. Zhang, L.C. Liu, Y. Xu, Y.C. Wang, D.L. Xu, A new alkali-activated steel slag-based cementitious material for photocatalytic degradation of organic pollutant from waste water, *J. Hazard. Mater.*, 209–210 (2012) 146–150.
- [34] L.E. Christianson, C. Lepine, P.L. Sibrell, C. Penn, S.T. Summerfelt, Denitrifying woodchip bioreactor and phosphorus filter pairing to minimize pollution swapping, *Water Res.*, 121 (2017) 129–139.
- [35] Z. Peng, H. Reti, Z. Dongkai, H.E. Yiqun, B. Zhiyuan, Synergism of novel sequence bio-ecological process and biological aerated filter for sewage treatment in cold climate, *Chin. J. Chem. Eng.*, 19 (2011) 881–890.
- [36] S.-Y. Liu, J. Gao, Y.-J. Yang, Y.-C. Yang, Z.-X. Ye, Adsorption intrinsic kinetics and isotherms of lead ions on steel slag, *J. Hazard. Mater.*, 173 (2010) 558–562.
- [37] S.-Y. Liu, J. Gao, B. Qu, Y.-J. Yang, X. Xin, Kinetic models for the adsorption of lead ions by steel slag, *Waste Manage. Res.*, 28 (2010) 748–753.
- [38] J.X. Tang, L.N. Sun, Y.P. Yun, M.M. He, M.H. Lian, Q. Luo, Adsorption of phosphate in aqueous solution with steel slag, *Appl. Mech. Mater.*, 522–524 (2014) 401–404.
- [39] D. Vukelic, N. Boskovic, B. Agarski, J. Radonic, I. Budak, S. Pap, M. Turk Sekulic, Eco-design of a low-cost adsorbent produced from waste cherry kernels, *J. Cleaner Prod.*, 174 (2018) 1620–1628.
- [40] M. Gupta, H. Gupta, D.S. Kharat, Adsorption of Cu(II) by low cost adsorbents and the cost analysis, *Environ. Technol. Innovation*, 10 (2018) 91–101.
- [41] X.Q. Huang, W.F. Wu, Y. Xia, W.B. Li, Y.Y. Gong, Z.J. Li, Alkali resistant nanocomposite gel beads as renewable adsorbents for water phosphate recovery, *Sci. Total Environ.*, 685 (2019) 10–18.
- [42] S. Ahmad, A. Ahmad, S. Khan, S. Ahmad, I. Khan, S. Zada, P.C. Fu, Algal extracts based biogenic synthesis of reduced graphene oxides (rGO) with enhanced heavy metals adsorption capability, *J. Ind. Eng. Chem.*, 72 (2019) 117–124.
- [43] W.D. Wu, J.H. Li, T. Lan, K. Müller, N.K. Niazi, X. Chen, S. Xu, L.R. Zheng, Y.C. Chu, J.W. Li, G.D. Yuan, H.L. Wang, Unraveling sorption of lead in aqueous solutions by chemically modified biochar derived from coconut fiber: a microscopic and spectroscopic investigation, *Sci. Total Environ.*, 576 (2017) 766–774.
- [44] H.-P. Mattila, H. Hudd, R. Zevenhoven, Cradle-to-gate life cycle assessment of precipitated calcium carbonate production from steel converter slag, *J. Cleaner Prod.*, 84 (2014) 611–618.
- [45] B.M. Mercado-Borrayo, R. Schouwenaars, J.L. González-Chávez, R.M. Ramírez-Zamora, Multi-analytical assessment of iron and steel slag characteristics to estimate the removal of metalloids from contaminated water, *J. Environ. Sci. Health. Part A Toxic/Hazard. Subst. Environ. Eng.*, 48 (2013) 887–895.
- [46] R.L. Gao, Q.L. Fu, H.Q. Hu, Q. Wang, Y.H. Liu, J. Zhu, Highly-effective removal of Pb by co-pyrolysis biochar derived from rape straw and orthophosphate, *J. Hazard. Mater.*, 371 (2019) 191–197.
- [47] J.J. Gallardo-Rodríguez, A.C. Rios-Rivera, M.R. Von Bennevit, Living biomass supported on a natural-fiber biofilter for lead removal, *J. Environ. Manage.*, 231 (2019) 825–832.
- [48] P. Bartczak, M. Norman, Ł. Klapiszewski, N. Karwańska, M. Kawalec, M. Baczyńska, M. Wysokowski, J. Zdarta, F. Ciesielczyk, T. Jesionowski, Removal of nickel(II) and lead(II) ions from aqueous solution using peat as a low-cost adsorbent: a kinetic and equilibrium study, *Arabian J. Chem.*, 11 (2018) 1209–1222.
- [49] M.Y. Kim, T.G. Lee, Removal of Pb(II) ions from aqueous solutions using functionalized cryogels, *Chemosphere*, 217 (2019) 423–429.
- [50] L.Y. Yang, T.T. Wen, L.P. Wang, T.H. Miki, H. Bai, X. Lu, H.F. Yu, T. Nagasaka, The stability of the compounds formed in the process of removal Pb(II), Cu(II) and Cd(II) by steelmaking slag in an acidic aqueous solution, *J. Environ. Manage.*, 231 (2019) 41–48.
- [51] B.M. Mercado-Borrayo, R. Contreras, A. Sánchez, X. Font, R. Schouwenaars, R.M. Ramírez-Zamora, Optimisation of the removal conditions for heavy metals from water: a comparison between steel furnace slag and CeO₂ nanoparticles, *Arabian J. Chem.*, 13 (2020) 1712–1719.
- [52] U. Kumarasinghe, K. Kawamoto, T. Saito, Y. Sakamoto, M.I.M. Mowjood, Evaluation of applicability of filling materials in permeable reactive barrier (PRB) system to remediate groundwater contaminated with Cd and Pb at open solid waste dump sites, *Process Saf. Environ. Prot.*, 120 (2018) 118–127.
- [53] D. Alexander, R. Ellerby, A. Hernandez, F.C. Wu, D. Amarasiriwardena, Investigation of simultaneous adsorption properties of Cd, Cu, Pb and Zn by pristine rice husks using ICP-AES and LA-ICP-MS analysis, *Microchem. J.*, 135 (2017) 129–139.
- [54] M.Y. Kim, T.G. Lee, Removal of Pb(II) ions from aqueous solutions using functionalized cryogels, *Chemosphere*, 217 (2019) 423–429.
- [55] A. Esrafil, S. Bagheri, M. Kermani, M. Gholami, M. Moslemzadeh, Simultaneous adsorption of heavy metal ions (Cu²⁺ and Cd²⁺) from aqueous solutions by magnetic silica nanoparticles (Fe₃O₄@SiO₂) modified using EDTA, *Desal. Water Treat.*, 158 (2019) 207–215.
- [56] Y.-H. Li, Z.C. Di, J. Ding, D.H. Wu, Z.K. Luan, Y.Q. Zhu, Adsorption thermodynamic, kinetic and desorption studies of Pb²⁺ on carbon nanotubes, *Water Res.*, 39 (2005) 605–609.
- [57] A. Behnamfard, M.M. Salarirad, Equilibrium and kinetic studies on free cyanide adsorption from aqueous solution by activated carbon, *J. Hazard. Mater.*, 170 (2009) 127–133.
- [58] W.S. Cha, J.W. Kim, H.C. Choi, Evaluation of steel slag for organic and inorganic removals in soil aquifer treatment, *Water Res.*, 40 (2006) 1034–1042.
- [59] E. Repo, J.K. Warchoł, L.J. Westholm, M. Sillanpää, Steel slag as a low-cost sorbent for metal removal in the presence of chelating agents, *J. Ind. Eng. Chem.*, 27 (2015) 115–125.
- [60] F. Liu, K.G. Zhou, Q.Z. Chen, A.H. Wang, W. Chen, Preparation of magnetic ferrite by optimizing the synthetic pH and its application for the removal of Cd(II) from Cd-NH₃-H₂O system, *J. Mol. Liq.*, 264 (2018) 215–222.

Supplementary Information

Table S1

Test tap water characterization

Ingredient	pH	TDS (mg L ⁻¹)	Na ⁺ (mg L ⁻¹)	Ca ⁺² (mg L ⁻¹)	Mg ⁺² (mg L ⁻¹)	Cl ⁻¹ (mg L ⁻¹)	Alkalinity (mg L ⁻¹)	Hardness (mg L ⁻¹)
Content %	7.2	1,150	186	285	25	280	122	195

Table S2

Surface characteristics adsorbent (BET)

Adsorbent	Surface area (m ² g ⁻¹)	Pore volume (cm ³ g ⁻¹)	Pore size (nm)
Steel slag	6.33	0.1 × 10 ⁻³	6.0
SAM-modified SS before use	62.82	3.6 × 10 ⁻³	50.0
SAM-modified SS after five cycle	58.12	3.0 × 10 ⁻³	42.0

Table S3

Test real wastewater characterization

Parameters	Initial concentration
pH	3.25–3.11
COD	494.08–505.76 mg L ⁻¹
Lead (Pb ⁺²)	208 mg L ⁻¹
Sodium (Na ⁺)	3.93 mg L ⁻¹
Potassium (K ⁺)	0.81 mg L ⁻¹
Calcium (Ca ⁺²)	3.58 mg L ⁻¹